OPEN

Interobserver Agreement Rates on C-X-C Motif Chemokine Receptor 4–Directed Molecular Imaging and Therapy

Philipp E. Hartrampf, MD, Aleksander Kosmala, MD,* Sebastian E. Serfling, MD,* Lena Bundschuh, MSc,† Takahiro Higuchi, MD, PhD,‡ Constantin Lapa, MD,† Steven P. Rowe, MD, PhD,§ Yohji Matsusaka, MD,* Alexander Weich, MD,||¶ Andreas K. Buck, MD,* Ralph A. Bundschuh, MD, PhD,† and Rudolf A. Werner, MD*§¶*

Background: We aimed to evaluate the interobserver agreement rates in patients scanned with C-X-C motif chemokine receptor 4 (CXCR4)–directed PET/CT, including the rate of patients eligible for CXCR4-targeted radioligand therapy (RLT) based on scan results.

Methods: Four independent observers reviewed 50 CXCR4-targeted [^{68}Ga]pentixafor PET/CT of patients with various solid cancers. On a visual level, the following items were assessed by each reader: overall scan impression, number of organ and lymph node (LN) metastases and number of affected organs and LN regions. For a quantitative investigation, readers had to choose a maximum of 3 target lesions, defined as largest in size and/or most intense uptake per organ compartment. Reference tissues were also quantified, including unaffected hepatic parenchyma and blood pool. Last, all observers had to decide whether patients were eligible for CXCR4-targeted RLT. Concordance rates were tested using intraclass correlation coefficients (ICCs). For interpretation, we applied the definition of Cicchetti (with 0.4–0.59 indicating fair; 0.6–0.74, good; 0.75–1, excellent agreement).

Results: On a visual level, fair agreement was achieved for an overall scan impression (ICC, 0.58; 95% confidence interval, 0.45–0.71). Organ and LN involvement (ICC, ≥0.4) demonstrated fair, whereas CXCR4 density and number of LN and organ metastases showed good agreement rates (ICC, ≥0.65). Number of affected organs and affected LN areas, however, showed excellent concordance (ICC, ≥0.76). Quantification in LN and organ lesions also provided excellent agreement rates (ICC, ≥0.92), whereas quantified uptake in reference organs provided fair concordance (ICC, ≥0.54). Again, excellent agreement rates were observed when deciding on patients eligible for CXCR4-RLT (ICC, 0.91; 95% confidence interval, 0.85–0.95).

Conclusions: In patients scanned with CXCR4-targeted PET/CT, we observed fair to excellent agreement rates for both molecular imaging and therapy parameters, thereby favoring a more widespread adoption of [^{68}Ga]pentixafor in the clinic.

Key Words: [^{68}Ga]pentixafor, C-X-C motif chemokine receptor 4, CXCR4, interobserver, radioligand therapy, theranostics

(*Clin Nucl Med* 2023;48: 483–488)

Overexpressed on various cancers, upregulation of C-X-C motif chemokine receptor 4 (CXCR4) portends a dismal prognosis[1,2] but has also emerged as a potential imaging and therapeutic target in recent years.[3] In this regard, the CXCR4-directed PET agent [^{68}Ga]pentixafor has previously been found to provide excellent image contrast among a broad range of malignancies.[4–6] Moreover, based on intensity and widespread disease (WD), the therapeutic equivalent [^{177}Lu/^{90}Y]pentixather has also achieved substantial outcome benefits in patients who have exhausted previous treatment options.[7,8] Beyond those image-guided selection strategies for CXCR4-directed radioligand therapies (RLTs), [^{68}Ga]pentixafor may also be useful to identify candidates that would be suitable for "cold" drugs also interacting with CXCR4, for example, small-molecule antagonists, peptides, or antibodies.[9,10] [^{68}Ga]pentixafor PET could then assess the retention capabilities of those drugs at baseline or in a longitudinal setting, thereby providing a more acceptable safety profile or even improve therapeutic efficacy if those therapeutics are administered.[11]

Before a more extensive use as a pan-tumor radiotracer, high interobserver agreement rates for CXCR4-directed molecular imaging and therapy are indispensable.[12] Such studies evaluating the concordance rates among multiple observers have already been conducted for multiple other theranostics radiotracers in the recent past, including agents targeting prostate-specific membrane antigen, cancer-associated fibroblasts, or somatostatin receptor,[13–15] but have not been performed for [^{68}Ga]pentixafor PET/CT. Thus, we aimed to provide agreement rates among multiple readers on a visual and quantitative level for both target lesions (TLs) and normal reference organs in patients with varying tumors imaged with [^{68}Ga]pentixafor. Last, we also assessed the agreement rates among readers as to what patients would have been suitable for CXCR4-directed RLT.

MATERIALS AND METHODS

General

We retrospectively investigated 50 patients affected with solid cancers, who had been imaged with [^{68}Ga]pentixafor to assist in diagnosis or

Received for publication November 28, 2022; revision accepted February 6, 2023.

From the *Department of Nuclear Medicine, University Hospital Würzburg, Würzburg; †Nuclear Medicine, Medical Faculty, University Hospital Augsburg, Augsburg, Germany; ‡Faculty of Medicine, Dentistry and Pharmaceutical Sciences, Okayama University, Okayama, Japan; §Johns Hopkins School of Medicine, The Russell H Morgan Department of Radiology and Radiological Sciences, Baltimore, MD; ||Internal Medicine II, Gastroenterology, University Hospital Würzburg; and ¶NET-Zentrum Würzburg, European Neuroendocrine Tumor Society Center of Excellence (ENETS CoE), University Hospital Würzburg, Würzburg, Germany.

Conflicts of interest and sources of funding: This project was partially supported by the Okayama University "RECTOR" Program, KAKENHI grant (21K19450) from the Japan Society for the Promotion of Science (T.H.) and the German Research Foundation (507803309, R.A.W.; 453989101, R.A.W., T.H.). R.A.W. and A.K.B. have received speaker's honoraria from PentixaPharm. A.K.B. is a member of the advisory board of PentixaPharm. R.A.B. is consultant to and has received speaker's honoraria from Bayer Healthcare (Leverkusen, Germany) and Eisai GmbH (Frankfurt, Germany). The other authors have no conflicts to report.

P.E.H., A.K., R.A.B., and R.A.W. contributed equally to this work.

Correspondence to: Rudolf A. Werner, MD, University Hospital Würzburg, Department of Nuclear Medicine, Oberdürrbacher Str. 6, 97080 Würzburg, Germany. E-mail: werner_r1@ukw.de.

ISSN: 0363-9762/23/4806–0483
DOI: 10.1097/RLU.0000000000004629

when conventional imaging provided inconclusive findings. All subjects provided written informed consent. The local ethics committee waived the need for further approval (no. 20210726 02). Of the 50 included patients, 17 (34%) were referred for staging, and the remaining 33 (66%) for restaging. Diagnoses included lung carcinoma (21/50 [42%]) and neuroendocrine neoplasms (NENs, 19/50 [38%]) in most cases, followed by hepatocellular carcinoma (8/50 [16%]) and pancreas carcinoma in the remaining 2 subjects (4%). For further details, refer to Table 1. Previous work also investigated parts of this cohort,[16–22] but without assessing interobserver agreement rates for molecular imaging and RLT in the context of CXCR4-targeted PET/CT.

Imaging Acquisition

As described by Serfling et al,[16] we conducted [^{68}Ga] pentixafor PET/CT on a Siemens Biograph mCT (64 or 128; Siemens Medical Solutions, Erlangen, Germany). One hour after tracer injection, whole-body scans covered the vertex of the skull to the thighs. Low-dose CTs were also performed for anatomical coregistration and attenuation correction.[23] Reconstruction of PET images included corrections for CT-based attenuation, random events, and scatter.[16]

Scan Interpretation

We used a syngo.via (VB50; Siemens Healthineers, Erlangen, Germany) workstation to read all PET/CTs. Four observers (minimum of 3 years' experience in reading PET/CTs) conducted image interpretation independently from each other and had no further clinical information, except for diagnosis, age, indication for scan, and prior therapies (Table 1). If readers were unfamiliar with the workstation, a brief training session was performed.[15]

On a visual level, we assessed an overall scan impression (positive/negative), with scans classified as positive in PETs displaying relevant radiotracer uptake in tumor sites above background. Such a binary rating was also applied for organ and lymph node (LN) involvement. We also evaluated the number of organs affected, the number of organ metastases, the number of affected LN areas, and the number of LN metastases applying a 5-point scale (ranging from 1 to ≥5 for each parameter). Uptake density, however, was scored on a 4-point scale (none, 0; low, 1; intermediate, 2; or high, 3).[15,24] Last, by assessing uptake intensity or WD, observers also decided whether CXCR4-directed RLT should be considered (including the portion of patients for whom both conditions [intensity, WD] would have been applicable to proceed with RLT).[15]

As described by Serfling et al,[15] we also conducted a quantitative assessment of TLs, which were defined as the largest in size and/or with the most intense uptake. No more than 3 metastases per organ compartment were identified and included the primary, lung, skeleton, liver, soft tissue, and LN. In this regard, the first 5 compartments were subsumed as organ lesions (OLs). For TLs, we recorded SUV_{max}. For reference organs, we used the blood pool derived from left ventricle and unaffected liver and quantified mean SUV.

TABLE 1. Patients Characteristics

Female		19/50 (38)
Age		63.7 ± 10.3*
Scan indication	Staging	17/50 (34)
	Restaging	33/50 (66)
Diagnosis	Lung carcinoma	21/50 (42)
	NENs	19/50 (38)
	Hepatocellular carcinoma	8/50 (16)
	Pancreas carcinoma	2/50 (4)
Therapies before scan	Chemotherapy	25/50 (50)
	Radiation therapy	12/50 (24)
	Surgery	10/50 (20)

*Mean ± SD. Percentages are given in brackets.

TABLE 2. Overview of ICCs (Single Measure) for Visual Assessment

Parameter	ICC
Overall scan result*	0.58 (0.45–0.71)
CXCR4 density in tumor tissue†	0.72 (0.61–0.81)
Organ involvement*	0.4 (0.25–0.55)
No. affected organs‡	0.76 (0.66–0.84)
No. organ metastases‡	0.74 (0.64–0.83)
LN involvement*	0.54 (0.4–0.67)
No. affected LN areas‡	0.78 (0.69–0.86)
No. LN metastases‡	0.65 (0.53–0.76)

Given in brackets are 95% CIs.

Assessed in a *binary fashion, on a †4-point or ‡5-point scale.

Statistical Analysis

We calculated intraclass correlation coefficients (ICCs, including 95% confidence intervals [CIs]), as described by Werner et al.[24] Agreement rates were then classified as follows: fair, 0.4 to 0.59; good, 0.6 to 0.74; excellent agreement, 0.75 to 1.[25] For statistical analysis, MedCalc statistical software (version 18.2.1; MedCalc Software bvba, Ostend, Belgium) was used.[26–28]

RESULTS

Fair to Excellent Interobserver Agreement Rates for Visual Assessment

For all parameters investigated in a binary fashion, fair agreement rates were achieved, including ratings for an overall scan impression (ICC, 0.58 [95% CI, 0.45–0.71]), LN (ICC, 0.54 [95% CI, 0.4–0.67]), and organ involvement (ICC, 0.4 [95% CI, 0.25–0.55]). Among items assessed on a 4- or 5-point scale, CXCR4 density (ICC, 0.72 [95% CI, 0.61–0.81]), number of LN (ICC, 0.65 [95% CI, 0.53–0.76]), and number of OLs (ICC, 0.74 [95% CI, 0.64–0.83]) achieved good agreement. Number of affected organs (ICC, 0.76 [95% CI, 0.66–0.84]) and affected LN areas (ICC, 0.78 [95% CI, 0.69–0.86]), however, showed excellent concordance rates (Table 2).

TABLE 3. Overview of ICCs (Single Measure) for Quantitative Parameters, Displayed by Organ Compartment

Compartment	ICC
OLs*	0.92 (0.87–0.96)
LN lesions	0.95 (0.92–0.98)
Blood pool	0.56 (0.42–0.69)
Unaffected liver	0.54 (0.4–0.67)

Sites of disease (organ or LN lesions) and reference tissues (blood pool, unaffected liver) were investigated quantitatively. For tumor sites, SUV_{max}, and for reference organs, SUV_{mean} were recorded. Given in brackets are 95% CIs.

*Includes TLs of the primary, lung, skeleton, liver, and soft tissue.

TABLE 4. Overview of ICCs for RLT Based on Intensity, Widespread Disease, or Both

Parameter	ICC
Intensity	0.66 (0.53–0.76)
Widespread disease	0.59 (0.46–0.72)
Intensity + WD	0.91 (0.85–0.95)

Given in brackets are 95% CIs.

Fair to Excellent Interobserver Agreement Rates for Quantitative Image Assessment

All readers identified 728 TLs, which were distributed among organ compartments as follows: LN (302/728 [41.5%]), primary (127/728 [17.4%]), liver (124/728 [17.0%]), skeleton (71/728 [9.8%]), lung (47/728 [6.5%]), and soft tissue (57/728 [7.8%]). The identical TL was chosen in 322 (44.2%) of 728 instances by all readers. Relative to a visual investigation, quantitative analyses yielded comparable findings. Investigating TLs, organ (ICC, 0.92 [95% CI, 0.87–0.96]), and LN lesions (ICC, 0.95 [95% CI, 0.92–0.98]) provided excellent concordance rates. Uptake on reference organs, however, provided fair agreement rates (blood pool: ICC, 0.56 [95% CI, 0.42–0.69]; unaffected liver: ICC, 0.54 [95% CI, 0.4–0.67]; Table 3).

Excellent Concordance for CXCR4-Targeted RLT

When readers had to decide on CXCR4-targeted RLT, a good agreement rate was just missed for WD (ICC, 0.59 [95% CI, 0.46–0.72]), but reached for intensity (ICC, 0.66 [95% CI, 0.53–0.76]). If both parameters were used to identify suitable candidates, concordance was then excellent (ICC, 0.91 [95% CI, 0.85–0.95]; Table 4).

Figure 1 provides a forest plot displaying ICCs along with 95% CI for all investigated items, whereas Figure 2 shows a patient affected with NEN, where all 4 observers decided on RLT based on intensity and WD.

DISCUSSION

Investigating subjects affected with solid tumors using the pan-tumor agent [^{68}Ga]pentixafor, we observed fair to excellent agreement rates on imaging assessments, including quantitative and visual analyses for both LN and organ metastases. Moreover, radiotracer accumulation in blood pool and unaffected hepatic parenchyma also achieved fair concordance rates, thereby indicating that both organs may be used to calculate target-to-background ratios (TBRs) for contrast evaluations. Last, when investigating suitable candidates for CXCR4-RLT based on imaging, excellent agreement rates were recorded. As such, [^{68}Ga]pentixafor is nearing readiness to be used in clinical routine or multi-institutional trials, as the molecular imaging expert or referring treating physician can

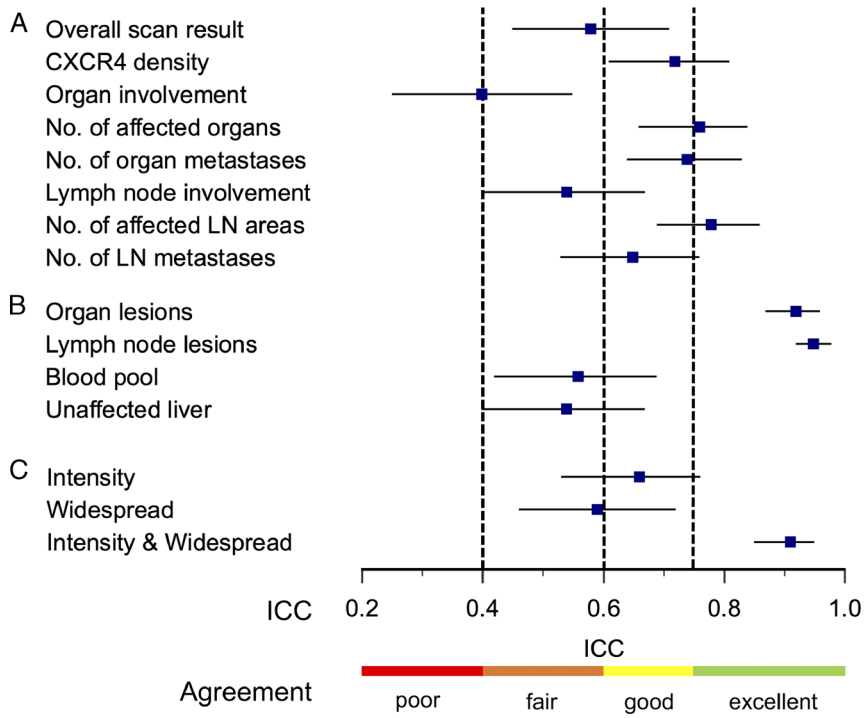

FIGURE 1. Forest plot with ICCs (including 95% CIs) for (**A**) visual interpretation, (**B**) quantitative evaluation, and (**C**) decision on CXCR4-directed RLT. On a visual assessment (**A**), all investigated parameters reached minimum fair agreement. Number of affected organs, organ metastases, affected LN areas, and LN metastases reached good concordance, which was also the case for CXCR4 density. On quantitative assessment (**B**), organ and LN metastases reached excellent agreement rates, whereas uptake assessments from normal hepatic parenchyma and blood pool demonstrated fair agreement. Investigating patients for CXCR4-RLT (**C**), fair agreement rates were recorded for deciding on treatment based on WD alone, whereas intensity alone achieved good concordance. Agreement rates, however, were excellent, when scans were rated based on both intensity and WD.

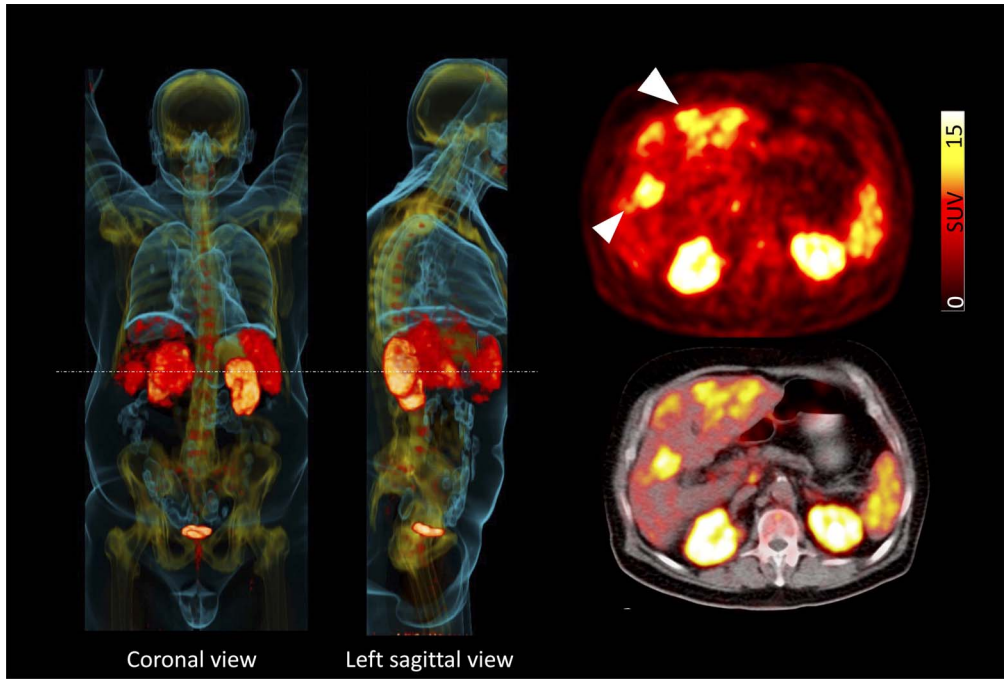

FIGURE 2. A 67-year old man affected with neuroendocrine carcinoma of the cardia (Ki-67, 90%), which was evaluated for CXCR4-directed RLT. Maximum intensity projections (coronal view, left; sagittal view, middle) and transaxial PET and PET/CT (right) showed intense CXCR4 expression (white arrows). All readers classified this patient eligible for CXCR4-targeted RLT based on both conditions (intensity and WD).

have a high certainty that multiple observers will not substantially deviate in their scan reports.

Similar to other theranostic radiotracers,[13–15] high concordance rates among multiple readers are needed to favor a more widespread adoption in the clinic, for both visual and quantitative evaluations.[12] Investigating a CXCR4-targeted PET agent, which has already been applied to various clinical scenarios in an oncology setting,[4–6,17] we observed ICC of at least 0.65 for the number of affected LN areas, number of LNs, number of affected organs, and number of OLs, thereby indicating that for both LN and visceral tumor spread concordance rates were at least good. Comparable ICCs have been observed for PET agents targeting somatostatin receptor or prostate-specific membrane antigen.[13,29,30] Of note, the latter studies investigated homogenous patient cohorts affected with either gastrointestinal NEN or prostate cancer, whereas in the present investigation, a broad range of varying tumor subtypes were included. Despite such a challenging scenario focusing not only on one single tumor entity, recorded ICCs were still high, a phenomenon that has also been observed for fibroblast activation protein inhibitor (FAPI) PET/CT.[15] As such, similar to FAPI-targeted imaging, [^{68}Ga]pentixafor may emerge as a pan-tumor radiotracer,[11] with multiple observers providing comparable scan reports. Moreover, in previous investigations, the concordance rates for other theranostics radiotracers were based on a guide for scan interpretation,[13] whereas our study applied a random TL investigation, with the intersecting set used for further analyses. Such a relatively unrestrictive approach, however, still led to high ICCs for LN and visceral metastases. Nonetheless, future studies may apply dedicated framework systems, which have been already established for other theranostic radiotracers[31–33] and which may further improve concordance among multiple observers reading [^{68}Ga]pentixafor PET/CT.

Serving as reference for TBR, we also assessed uptake in the blood pool and unaffected hepatic parenchyma. Derived ratios, however, are of importance to evaluate image contrast, with higher ratios indicating that tumor sites can be more reliably identified when compared with physiological biodistribution.[17] In this regard, we observed again substantial agreement rates for both organs. As a possible explanation for the relatively low ICC in the blood derived from the left ventricle, previous reports have already demonstrated that remote (unaffected) cardiac segments (distant from infarcted myocardium) also exhibit varying CXCR4 expression in vivo.[34] In addition, a relatively broad range of SUV was also observed for both the blood pool derived from the heart and unaffected liver parenchyma in a previous study investigating uptake in normal organs after [^{68}Ga]pentixafor injection.[16] Taken together, those previously shown findings may also partially explain the relatively low ICCs of the present investigation for both blood pool and liver. Nonetheless, we observed excellent concordance for quantified uptake in LN and OL, which may be relevant for an accurate read-out of tumor manifestations, but also for a reliable assessment of the retention capacities in vivo, for example, for "cold" CXCR4 inhibitory drugs.[35] Moreover, the (quantified) intratumoral lesion variability among multiple observers was higher on FAPI-targeted PET/CT when compared with the present findings on SUV_{max} for [^{68}Ga]pentixafor.[35] As a possible explanation, substantial and consistent CXCR4 upregulation has already been described in an ex vivo setting for both aggressive lung cancer and NEN.[36,37] As we also enrolled mainly those tumor types, those previous immunohistochemical findings may partially explain the high concordance rates of minimum 0.92 for TLs.

Last, we also observed excellent agreement rates when identifying patients eligible for CXCR4 RLT. In a theranostic setup, administration of the therapeutic compound not only achieves an

antilymphoma effect, but also causes bone marrow ablation.[7,8] As such, after waiting for decay in the stem cell niche, patients can then be scheduled for subsequent stem cell transplantation.[11] Although this may be desired for theranostics in hemato-oncology,[11] such an approach would be classified as a relevant off-target effect if CXCR4 RLT would be conducted in solid malignancies. Nonetheless, the herein observed fair to excellent agreement rates are of relevance, for example, if patients are risk-stratified for "cold" CXCR4-directed therapy based on imaging, including peptides or antibodies.[9,10] Moreover, investigating a large cohort of patients affected with hematologic malignancies, the highest SUV_{max} and TBR have been recorded in subjects with different lymphoma subtypes or multiple myeloma.[17] Thus, the herein presented study concept may serve as a template to investigate the concordance rates in patients with advanced blood cancers. Further limitations include the retrospective design and the overall low number of investigated patients or metastases. Nonetheless, we identified 322 TLs, which were seen by all 4 observers. Of note, prospective studies using CXCR4-PET/CT and RLT are currently initiated,[38] which may then corroborate our initial results on the interobserver agreement rates in patients imaged with [^{68}Ga]pentixafor PET/CT. Last, in the present blinded reads, lower agreement was achieved on judging organ and LN involvement on a visual basis with reaching only fair concordance (Fig. 1), whereas reasons for major disagreement were not recorded. Those may include different levels of previous experience, tissue type, or investigated tumor entity, and future studies on interobserver agreement rates in the context of CXCR4-directed PET/CT may then also document those findings on a reader-based level.

CONCLUSIONS

We observed fair to excellent concordance rates in patients imaged with CXCR4-targeted PET/CT for both visual and quantitative assessments, with high ICCs achieved for quantification in sites of disease. Those excellent agreement rates were also recorded for identifying subjects eligible for CXCR4 RLT based on molecular imaging. Taken together, the herein observed concordance may lay the foundation for more widespread use of [^{68}Ga]pentixafor in the clinic and for multi-institutional trials.

REFERENCES

1. Zhao H, Guo L, Zhao H, et al. CXCR4 over-expression and survival in cancer: a system review and meta-analysis. *Oncotarget*. 2015;6: 5022–5040.
2. Lewis R, Maurer HC, Singh N, et al. CXCR4 hyperactivation cooperates with TCL1 in CLL development and aggressiveness. *Leukemia*. 2021;35: 2895–2905.
3. Walenkamp AME, Lapa C, Herrmann K, et al. CXCR4 ligands: the next big hit? *J Nucl Med*. 2017;58:77S–82S.
4. Mayerhoefer ME, Raderer M, Lamm W, et al. CXCR4 PET imaging of mantle cell lymphoma using [(68)Ga]Pentixafor: comparison with [(18)F] FDG-PET. *Theranostics*. 2021;11:567–578.
5. Mayerhoefer ME, Raderer M, Lamm W, et al. CXCR4 PET/MRI for follow-up of gastric mucosa–associated lymphoid tissue lymphoma after first-line *Helicobacter pylori* eradication. *Blood*. 2022;139: 240–244.
6. Herhaus P, Lipkova J, Lammer F, et al. CXCR4-targeted PET imaging of central nervous system B-cell lymphoma. *J Nucl Med*. 2020;61: 1765–1771.
7. Habringer S, Lapa C, Herhaus P, et al. Dual targeting of acute leukemia and supporting niche by CXCR4-directed theranostics. *Theranostics*. 2018;8: 369–383.
8. Buck AK, Grigoleit GU, Kraus S, et al. C-X-C motif chemokine receptor 4–targeted radioligand therapy in patients with advanced T-cell lymphoma. *J Nucl Med*. 2022;64:34–39.
9. Sokkar P, Harms M, Sturzel C, et al. Computational modeling and experimental validation of the EPI-X4/CXCR4 complex allows rational design of small peptide antagonists. *Commun Biol*. 2021;4:1113.
10. Broussas M, Boute N, Akla B, et al. A new anti-CXCR4 antibody that blocks the CXCR4/SDF-1 axis and mobilizes effector cells. *Mol Cancer Ther*. 2016;15:1890–1899.
11. Buck AK, Serfling SE, Lindner T, et al. CXCR4-targeted theranostics in oncology. *Eur J Nucl Med Mol Imaging*. 2022;49:4133–4144.
12. Werner RA, Bundschuh RA, Bundschuh L, et al. Novel structured reporting systems for theranostic radiotracers. *J Nucl Med*. 2019;60: 577–584.
13. Fendler WP, Barrio M, Spick C, et al. ^{68}Ga-DOTATATE PET/CT Interobserver agreement for neuroendocrine tumor assessment: results of a prospective study on 50 patients. *J Nucl Med*. 2017;58:307–311.
14. Fendler WP, Calais J, Eiber M, et al. Assessment of ^{68}Ga-PSMA-11 PET accuracy in localizing recurrent prostate cancer: a prospective single-arm clinical trial. *JAMA Oncol*. 2019;5:856–863.
15. Serfling SE, Hartrampf PE, Zhi Y, et al. Interobserver agreement rates on fibroblast activation protein inhibitor–directed molecular imaging and therapy. *Clin Nucl Med*. 2022;47:512–516.
16. Serfling SE, Lapa C, Dreher N, et al. Impact of tumor burden on Normal organ distribution in patients imaged with CXCR4-targeted [(68)Ga]Gapentixafor PET/CT. *Mol Imaging Biol*. 2022;24:659–665.
17. Buck AK, Haug A, Dreher N, et al. Imaging of C-X-C motif chemokine receptor 4 expression in 690 patients with solid or hematologic neoplasms using (68)Ga-pentixafor PET. *J Nucl Med*. 2022;63:1687–1692.
18. Werner RA, Kircher S, Higuchi T, et al. CXCR4-directed imaging in solid tumors. *Front Oncol*. 2019;9:770.
19. Lapa C, Luckerath K, Rudelius M, et al. [^{68}Ga]Pentixafor-PET/CT for imaging of chemokine receptor 4 expression in small cell lung cancer—initial experience. *Oncotarget*. 2016;7:9288–9295.
20. Weich A, Werner RA, Buck AK, et al. CXCR4-directed PET/CT in patients with newly diagnosed neuroendocrine carcinomas. *Diagnostics (Basel)*. 2021;11:605.
21. Werner RA, Weich A, Schirbel A, et al. Intraindividual tumor heterogeneity in NET—further insight by C-X-C motif chemokine receptor 4–directed imaging. *Eur J Nucl Med Mol Imaging*. 2017;44:553–554.
22. Werner RA, Weich A, Higuchi T, et al. Imaging of chemokine receptor 4 expression in neuroendocrine tumors—a triple tracer comparative approach. *Theranostics*. 2017;7:1489–1498.
23. Kosmala A, Serfling SE, Schlotelburg W, et al. Impact of ^{68}Ga-FAPI-04 PET/CT on staging and therapeutic management in patients with digestive system tumors. *Clin Nucl Med*. 2022;48:35–42.
24. Werner RA, Derlin T, Rowe SP, et al. High interobserver agreement for the standardized reporting system SSTR-RADS 1.0 on somatostatin receptor PET/CT. *J Nucl Med*. 2021;62:514–520.
25. Cicchetti DV. Guidelines, criteria, and rules of thumb for evaluating normed and standardized assessment instruments in psychology. *Psychol Assess*. 1994;6:284–290.
26. *R Core Team, R: A Language and Environment for Statistical Computing*. Vienna, Austria; 2019. Available at: https://www.R-project.org/: R Foundation for Statistical Computing. Accessed November 1, 2022.
27. Gamer M, Lemon J, Singh IFP. *irr: Various Coefficients of Interrater Reliability and Agreement. R Package Version 0.84.1*. Vienna, Austria; 2019. Available at: https://CRAN.R-project.org/package=irr: R Foundation for Statistical Computing. Accessed November 1, 2022.
28. Canty A, Ripley B. *boot: Bootstrap R (S-Plus) Functions. R Package Version 1.3–23*. Vienna, Austria: R Foundation for Statistical Computing; 2019.
29. Fendler WP, Calais J, Allen-Auerbach M, et al. (68)Ga-PSMA-11 PET/CT interobserver agreement for prostate cancer assessments: an international multicenter prospective study. *J Nucl Med*. 2017;58:1617–1623.
30. Chavoshi M, Mirshahvalad SA, Metser U, et al. (68)Ga-PSMA PET in prostate cancer: a systematic review and meta-analysis of the observer agreement. *Eur J Nucl Med Mol Imaging*. 2022;49:1021–1029.
31. Ceci F, Oprea-Lager DE, Emmett L, et al. E-PSMA: the EANM standardized reporting guidelines v1.0 for PSMA-PET. *Eur J Nucl Med Mol Imaging*. 2021;48:1626–1638.
32. Eiber M, Herrmann K, Calais J, et al. Prostate Cancer Molecular Imaging Standardized Evaluation (PROMISE): proposed miTNM classification for the interpretation of PSMA-ligand PET/CT. *J Nucl Med*. 2018; 59:469–478.

33. Werner RA, Thackeray JT, Pomper MG, et al. Recent updates on Molecular Imaging Reporting and Data Systems (MI-RADS) for theranostic radiotracers-navigating pitfalls of SSTR- and PSMA-targeted PET/CT. *J Clin Med*. 2019;8.

34. Werner RA, Hess A, Koenig T, et al. Molecular imaging of inflammation crosstalk along the cardio-renal axis following acute myocardial infarction. *Theranostics*. 2021;11:7984–7994.

35. Zhao R, Liu J, Li Z, et al. Recent advances in CXCL12/CXCR4 antagonists and nano-based drug delivery systems for cancer therapy. *Pharmaceutics*. 2022;14.

36. Kaemmerer D, Trager T, Hoffmeister M, et al. Inverse expression of somatostatin and CXCR4 chemokine receptors in gastroenteropancreatic neuroendocrine neoplasms of different malignancy. *Oncotarget*. 2015;6:27566–27579.

37. Qiu L, Xu Y, Xu H, et al. The clinicopathological and prognostic value of CXCR4 expression in patients with lung cancer: a meta-analysis. *BMC Cancer*. 2022;22:681.

38. Menda Y. A Safety Study of 212Pb-Pentixather Radioligand Therapy. NCT05557708. Available at: https://clinicaltrials.gov/ct2/show/NCT05557708. Accessed March 15, 2023.